APPLIED ORGANOMETALLIC CHEMISTRY
Appl. Organometal. Chem. 2001; **15**: 593–603
DOI: 10.1002/aoc.205

Di-*n*-butyltin(IV) derivatives of bis(carboxymethyl)benzylamines: synthesis, NMR and X-ray structure characterization and *in vitro* antitumour properties

Teresa Mancilla,[1]* Lourdes Carrillo,[1] Luis S. Zamudio Rivera,[1] Carlos Camacho Camacho,[2]† Dick de Vos,[3] Robert Kiss,[4] Francis Darro,[5] Bernard Mahieu,[6] Edward R. T. Tiekink,[7] Hubert Rahier,[8] Marcel Gielen,[2]** Martine Kemmer,[2] Monique Biesemans[2] and Rudolph Willem[2]

[1]Centro de Investigación y de Estudios Avanzados del Instituto Politécnico Nacional, Department of Chemistry, Apdo. Postal 14-740, México D.F., 07000 Mexico
[2]Free University of Brussels (VUB), Department of General and Organic Chemistry, Faculty of Applied Sciences and High Resolution NMR Centre, Pleinlaan 2, B-1050 Brussels, Belgium
[3]PCH Nederland, Pharmachemie BV, Medical Department, PO Box 552, NL-003 RN Haarlem, The Netherlands
[4]Free University of Brussels (ULB), Faculty of Medicine, Laboratory of Histopathology, CP 620, Route de Lennik, 808, B-1070 Brussels, Belgium
[5]Centre de Recherches, Laboratoire Lafon, 19 avenue du Pr. Cadiot, F-94701 Maisons-Alfort, France
[6]Université Catholique de Louvain, Unité CPMC, Bâtiment Lavoisier, Place Pasteur, B-1348 Louvain-la-Neuve, Belgium
[7]Department of Chemistry, The University of Adelaide, 5005 Adelaide, Australia
[8]Free University of Brussels (VUB), Department of Physical and Polymer Chemistry, Faculty of Applied Sciences, Pleinlaan 2, B-1050 Brussels, Belgium

Four di-*n*-butyltin(IV) derivatives of bis(carboxymethyl)benzylamines were synthesized and their structure characterized by ^{1}H, ^{13}C and $^{117/119}Sn$ NMR, Mössbauer spectroscopy and mass spectrometry. The derivative substituted in the meta position by a methyl group has been further characterized by X-ray crystallography. This compound exhibits a distorted trigonal bipyramidal geometry at tin. The NMR data in solution, as well as other spectroscopic results in the solid state, confirm this structure for all the compounds. Evidence is provided to show that the compounds are more highly associated in concentrated solution than in the solid state. Their *in vitro* antitumour activity is reported.

Keywords: butyltin; benzylamines; structure; NMR; Mössbauer; mass spectroscopy

Received 9 August 2000; accepted 9 January 2001

* Correspondence to: T. Mancilla, Universidad Autónoma Metropolitana. Unidad Xochimilco, Departamento de Sistemas Biológicos, Calzada del Hueso 1100, Col. Villa Quietud, México D.F., 04960 Mexico.
** Correspondence to: M. Gielen, Free University of Brussels (VUB), Department of General and Organic Chemistry, Faculty of Applied Sciences and High Resolution NMR Centre, Pleinlaan 2, B-1050 Brussels, Belgium.
† Present address: Universidad Autónoma Metropolitana, Unidad Xochimilco, Departamento de Sistemas Biológicas, Calzada del Hueso 1100, Col. Villa Quietud, México DF, 04960 Mexico.
Contract/grant sponsor: Consejo Nacional de Ciencia y Tecnología (Conacyt); Contract/grant number: G32710E; Contract/grant number: 32198E.
Contract/grant sponsor: Fund for Scientific Research Flanders (Belgium); Contract/grant number: G.0192.98; Contract/grant number: G.0074.00.
Contract/grant sponsor: Ministère de l'Education National du Luxembourg; Contract/grant number: BF293/051; Contract/grant number: BPu96/130; Contract/grant number: BPu97/138; Contract/grant number: BPu98/071.
Contract/grant sponsor: Action "Vaincre le Cancer du Luxembourg".
Contract/grant sponsor: Australian Research Council.

1. INTRODUCTION

Many organotin(IV) compounds exhibit antitumour activity.[1–5] However, diorganotin(IV) derivatives

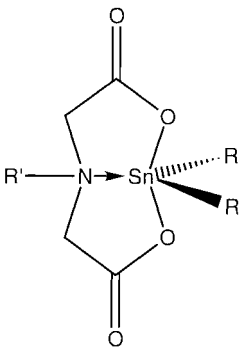

Ia: R' = H R = $CH_2(CH_2)_2CH_3$
Ib: R' = H R = $CH_2(CH_2)_6CH_3$
Ic: R' = H R = $CH_2C_6H_5$
Id: R' = CH_3 R = CH_3
Ie: R' = CH_3 R = CH_2CH_3
If: R' = CH_3 R = $CH_2(CH_2)_2CH_3$
Ig: R' = CH_3 R = $C(CH_3)_3$
Ih: R' = CH_3 R = $CH_2(CH_2)_6CH_3$
Ii: R' = CH_3 R = CH_2CONH_2
Ij: R' = CH_3 R = CH_2CH_2OH

Scheme 1

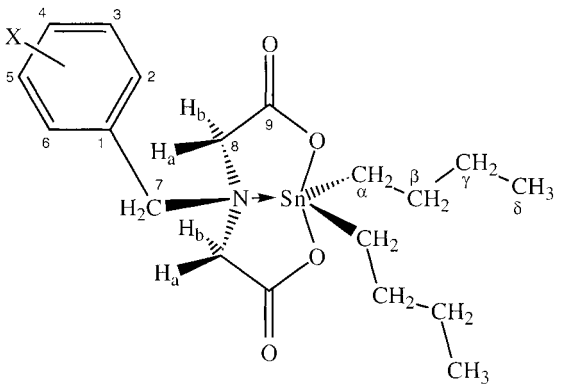

1: X = H; 2: X = o-CH_3; 3 : X = m-CH_3; 4: X = p-CH_3

Scheme 2

of bis(carboxymethyl)amines and some *N*-substituted analogues have been investigated only to a limited extent.[6,7] This is probably due to the fact that only some ligands are commercially available and methods for their preparation are not numerous.[8–10] Several papers deal with complexes of various metals containing the carboxylates of iminodiacetic acid, *N*-methyliminodiacetic acid and some other *N*-substituted iminodiacetic acids as main ligands.[7,11–19]

Among the compounds of Scheme 1,[6,7,19] **Ia** and **Ib** did not exhibit any activity *in vivo* against P388 leukaemia.[6] Compounds **Ia, If, Ih, Ii** and **Ij** have been tested *in vitro* against two human cell lines, MCF-7, a mammary tumour, and WiDr, a colon carcinoma. Except for **Ih**, these compounds display a high antitumour activity since they have significantly lower inhibition doses ID_{50} than *cis*-platin against both cell lines.[7,20]

We are interested in the chemistry and antitumour activity of tin complexes derived from ligands of this type. In this paper, we report the synthesis, structure and properties of a novel di-*n*-butyltin(IV) derivative of bis(carboxymethyl)benzylamine and its three analogues substituted by a methyl group on the phenyl moiety, compounds **1–4** (Scheme 2).[21]

The X-ray crystal structure of **3** has been determined. The solution- and solid-state structures of these compounds have been further addressed by ^{1}H, ^{13}C and ^{117}Sn NMR spectroscopy, as well as by ^{119m}Sn Mössbauer, IR spectroscopy and mass spectrometry. Their *in vitro* antitumour activity is reported.

2. RESULTS AND DISCUSSION

2.1 Synthesis

Compounds **1–4** were synthesized from the corresponding dicarboxylic acid and di-*n*-butyltin oxide with elimination of water. Crystals of **3** suitable for X-ray diffraction analysis were obtained by slow evaporation of a methylene chloride/heptane solution.

2.2 NMR data and structure

The ^{1}H NMR spectra of compounds **1–4** exhibit the expected resonances (Table 1), with an anisochrony for the diastereotopic CH_aH_bCOO protons. This finding shows that the tin atom is involved in a rigid and non-planar bicyclic framework (Scheme 2) due to the transannular nitrogen to tin coordination bond, with the tin atom adopting a distorted trigonal bipyramidal geometry. In all cases, $^{3}J(^{1}H–^{119/117}Sn)$ coupling satellites are observed for the H8a but not for the H8b protons. No $^{3}J(^{1}H–^{119/117}Sn)$ coupling satellites were observed for the H7 proton in the standard ^{1}H NMR spectrum, but $^{1}H–^{119}Sn$ correlation peaks were observed in the $^{1}H–^{119}Sn$ HMQC (Heteronuclear Multiple Quantum Coherence) spectrum for the H7 proton and

Table 1 ^{1}H NMR data of compounds **1–4** in $CDCl_3$

	1	**2**	**3**	**4**
	7.19 (d, 6): H2, H6 7.32–7.44 (m): H3, H4, H5	7.16–7.43 (m): H3, H4, H5, H6	7.02 (*): H2, H6 7.25 (d, 7): H4 7.31 (dd, 7, 7): H5	7.17 (d, 6): H2, H6 7.06 (d, 6): H3, H5
H7	4.03 (s)	4.13 (s)	3.99 (s)	3.98 (s)
H8a	3.94 (d, 16) [58/55]	3.94 (d, 16) [58]	3.97 (d, 16) [59/57]	3.93 (d, 16) [59]
H8b	2.98 (d, 16)	2.99 (d, 16)	2.98 (d, 16)	2.96 (d, 16)
CH_3	–	2.40 (s)	2.40 (s)	2.39 (s)
Hα, Hβ	1.53–1.77 (m) 1.80–1.95 (m)	1.54–1.78 (m) 1.83–1.92 (m)	1.52–1.75 (m) 1.82–1.91 (m)	1.55–1.75 (m) 1.81–1.90 (m)
Hγ	1.33–1.55 (m)	1.32–1.54 (m)	1.33–1.55 (m)	1.32–1.50 (m)
Hδ	0.94 (t, 7) 0.98 (t, 7)	0.94 (t, 7) 0.98 (t, 7)	0.94 (t, 7) 0.98 (t, 7)	0.94 (t, 7) 0.98 (t, 7)

Data obtained at 250.13 MHz. Chemical shifts in ppm with respect to TMS; coupling constants in hertz, $^{n}J(^{1}H–^{1}H)$ in parentheses; $^{n}J(^{1}H–^{119/117}Sn)$ coupling constants between square brackets.
Abbreviations: s = singlet; d = doublet; t = triplet; m = complex pattern. (*): expected doublet (H6) hidden by overlapping with a broad singlet (H2). Compound **1** (500.13 MHz): *n*-butyl 1: Hα: 1.87; Hβ: 1.87; Hγ: 1.49; Hδ: 0.98; *n*-butyl 2: Hα': 1.62; Hβ': 1.68; Hγ': 1.38; Hδ': 0.94 as obtained from 2D NOESY and TOCSY NMR spectra.

with much lower intensity for the H8b one. For compound **1**, the H8b and the H7 proton resonances exhibit intense cross-peaks with α and β *n*-butyl CH_2 resonances in the 2D NOESY (Nuclear Overhauser Enhancement Spectroscopy) spectrum, whereas those of the H8a protons do so with much lower intensity. This assigns spatially the H8b protons to a closer position with respect to the *n*-butyl groups' protons of the tin atom than the H8a protons. The value of the dihedral angle between the H8b and tin atoms obtained by molecular mechanics and semi-empirical methods[22] showed a value between 80 and 90 °, which explains why the coupling constant ^{3}J(H8b–$^{119/117}$Sn) is negligibly small. In addition, the 2D NOESY[23] and off-resonance ROESY (Rotating Frame Overhauser Enhancement Spectroscopy)[24] spectra exhibit pairwise exchange cross-peaks between *n*-butyl proton resonances, indicating chemical exchange of the *n*-butyl groups. This observation is in agreement with a mechanism in which the nitrogen—tin bond is broken, the pyramidal nitrogen inverted, and the nitrogen—tin bond regenerated,[19] and which eventually results in the chemical environments of the *n*-butyl groups being permutated. The assignment of the aromatic and *n*-butyl proton resonances was based on $^{1}H–^{13}C$ HMQC and HMBC (Heteronuclear Multiple Bond Correlation) experiments. In standard ^{1}H spectra, the *n*-butyl protons exhibit a complex pattern for the diastereotopic *n*-butyl groups. Because of overlapping and broad lines related to the exchange, no unambiguous spatial assignment can be proposed for the protons of these groups. However, for compound **1** the NOESY and TOCSY (Total Correlation Spectroscopy) spectra at 500 MHz enabled an *n*-butyl-specific assignment of the protons (see Table 1). The latter should also apply to compounds **2–4**, given the high ^{1}H chemical shift similarity. The chemical shifts of the aromatic protons of compound **1** are similar to those of *N*-protonated benzylamines.[25]

The ^{13}C NMR data of compounds **1–4** are reported in Table 2. For all compounds the assignment of the *n*-butyl and aromatic moieties are again based on the $^{1}H–^{13}C$ HMQC and $^{1}H–^{13}C$ HMBC experiments. The assignments were cross-checked with aromatic ^{13}C chemical shifts calculated using the increments deduced from the ^{13}C NMR data of **1** and toluene. The α-carbon atoms of the two *n*-butyl groups as well as the γ and δ carbon atoms in **3** and **4** have pairwise different ^{13}C chemical shifts, confirming that they are diastereotopic, in conformity with the structure proposed, with the β ^{13}C resonances being accidentally

Table 2 ^{13}C NMR data in $CDCl_3$

	1	**2**	**3**	**4**
C1	126.9	126.3 (b)(127.6)	126.8 (126.8)	123.9 (124.0)
C2	133.3	139.7 (b)(142.6)	133.8 (134.0)	133.2 (133.2)
C3	130.0	130.7 (b)(130.7)	140.1 (139.3)	130.7 (130.7)
C4	130.9	132.4 (b)(130.8)	131.8 (131.6)	141.2 (140.3)
C5	130.0	127.2 (127.1)	129.9 (129.9)	130.7 (130.7)
C6	133.3	134.0 (133.1)	130.4 (130.4)	133.2 (133.2)
C7	57.8	56.4	57.8	57.5
C8	55.9	54.6 (b)	55.9	55.9
C9	169.4 [18]	170.2	169.4 [18]	169.5 [18]
CH_3	–	20.2	21.9	21.8
Cα	22.8 [604/581]	23.1 (b)	22.8 [583/560]	22.7 [602/579]
Cα'	22.4 [ca 540]	23.1 (b)	22.4 [539/517]	22.4 [557/532]
Cβ, Cβ'	27.4 [25]	27.5 [26]	27.4 [27]	27.4 [25]
Cγ	27.3 [96]	27.3 [98]	27.4 [102/96]	27.3 [99]
Cγ'			27.3 [95/91]	27.2 [90]
Cδ	14.0	14.0	14.0	14.0
Cδ'			13.9	13.9

Chemical shifts in ppm with respect to TMS; $^{n}J(^{13}C–^{119/117}Sn)$ coupling constants between square brackets. Chemical shifts calculated from aromatic chemical shift increments of compound **1** and toluene are given in parentheses; b = broad.

isochronous. The $^{1}J(^{13}C–^{119/117}Sn)$ coupling constants, significantly different for the diastereotopic *n*-butyl groups, have orders of magnitude that also conform to the structure proposed.[26] The ^{117}Sn NMR data reveal interesting structural features (Table 3). The ^{117}Sn isotropic chemical shifts in the

Table 3 ^{117}Sn chemical shifts ($CDCl_3$)

		Solution (303 K)			
	Solid state	diluted	concentrated	Solution (213 K)	
1	−109	−118.3	−127.5	−115.0;	−282.5
				−322.9	
				−324.7	
				−330.2	
				−333.6	
2	−108	−117.9	−129.4	−110 (b);	−321.3
				−318.5	
				−321.3	
				−327.1	
				−329.8	
3	−108	−117.5	−124.1	−115 (b);	−281.4
				−321.5	
				−323.0	
				−328.7	
				−332.0	
4	−108	−118.0	−128.4	−117 (b);	−283.4
				−323.3	
				−325 (sh)	
				−330.0	
				−334.1	

Diluted: 20 mg/0.5 ml; concentrated: 100 mg/0.5 ml; b = broad; sh = overlapping shoulder; ^{117}Sn NMR chemical shifts in ppm with respect to $\Xi^{117}Sn = 35.632295$.

Table 4 ^{119m}Sn Mössbauer parameters of compounds **1–4**

Compound	IS (mm s^{-1})	QS (mm s^{-1})
1	1.34	3.30
2	1.35	3.48
3	1.33	3.11
4	1.33	3.05

QS (quadrupole splitting), IS (isomer shift) relative to $Ca^{119}SnO_3$.

solid state, around −108 ppm for all compounds, are characteristic for five-coordination, as are the ^{117}Sn chemical shifts for the diluted solution at hardly lower frequency. These data are in agreement with the monomeric structure as shown in Scheme 2 and exclude aggregation in the solid state. This conclusion was confirmed subsequently on the basis of a single-crystal X-ray diffraction study presented below. The solution ^{117}Sn chemical shifts move slightly to lower frequency upon fivefold concentration increase, which indicates a dynamic equilibrium, fast on the NMR time scale, between the above monomeric form and some aggregated species.[27] Lowering the temperature from 303 to 213 K confirms this proposal, as the single ^{117}Sn resonance decoalesces into several signals. For all four compounds, the low-temperature spectrum, from either the diluted or the concentrated solution, comprises: (i) a residual signal (*ca* 15%) in the range −110 to −117 ppm, characteristic for the five-coordinate species of Scheme 2; (ii) a more intense signal (*ca* 35%) around −282 ppm (−321 ppm for **2**), which indicates a coordination expansion through aggregation to a structure with only one type of tin; this suggests a dimer of the type previously described,[27] where the O—Sn oxygen coordinates a neighbouring tin with generation of a four-membered Sn_2O_2 cyclic core; (iii) a set of four equally intense resonances (*ca* 50% in total) in the range −320 to −335 ppm, suggesting the existence of an additional species in more aggregated form, necessarily at least a tetramer, with four diastereotopic tin atoms, probably due to the low symmetry of the monomeric unit. These temperature-dependent changes observed in the spectra are fully reversible. Note the shielding effect (40 ppm) of the ortho methyl groups of **2** on the ^{117}Sn chemical shift of the dimeric species.

2.3 Mössbauer data

The Mössbauer parameters of compounds **1–4** are given in Table 4. Quadropole Splitting (QS) values are in the range 2.1–2.4 mm s^{-1} for tetrahedral diorganotin compounds, 3.0–4.1 mm s^{-1} for trigonal bipyramidal compounds, 1.7–2.2 mm s^{-1} and 3.5–4.2 mm s^{-1} for *cis* and *trans* octahedral six-coordinate compounds respectively.[28] A comparison of these value ranges with the experimental data (Table 4) leads to the conclusion that, in the solid state, compounds **1–4** are five-coordinate, in line with the ^{117}Sn cross-polarization–magic angle

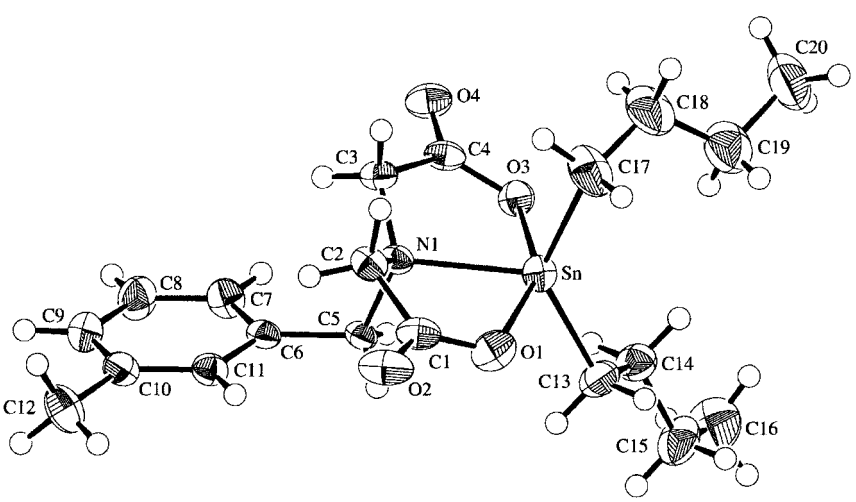

Figure 1 Molecular structure of **3** showing the crystallographic numbering scheme employed.

Table 5 Selected interatomic parameters (Å, deg) for **3**

Atoms	Parameter	Atoms	Parameters
Sn—O(1)	2.144(3)	Sn—O(3)	2.129(3)
Sn—N(1)	2.228(3)	Sn—C(13)	2.114(5)
Sn—C(17)	2.129(5)	C(1)—O(1)	1.288(5)
C(1)—O(2)	1.217(5)	C(4)—O(3)	1.301(5)
C(4)—O(4)	1.210(5)	N(1)—C(2)	1.480(5)
N(1)—C(3)	1.490(5)	N(1)—C(5)	1.525(5)
O(1)—Sn—O(3)	150.9(1)	O(1)—Sn—N(1)	75.4(1)
O(1)—Sn—C(13)	93.9(2)	O(1)—Sn—C(17)	95.8(2)
O(3)—Sn—N(1)	75.9(1)	O(3)—Sn—C(13)	96.5(1)
O(3)—Sn—C(17)	97.0(2)	N(1)—Sn—C(13)	119.7(2)
N(1)—Sn—C(17)	107.9(2)	C(13)—Sn—C(17)	132.3(2)
Sn—O(1)—C(1)	117.6(3)	Sn—O(3)—C(4)	117.9(2)
Sn—N(1)—C(2)	104.7(2)	Sn—N(1)—C(3)	106.4(2)
Sn—N(1)—C(5)	107.4(2)		

spinning (CP-MAS) NMR spectra. The QS values below 3.5 mm s^{-1} and above 2.2 mm s^{-1} exclude a dimeric structure with *trans* or *cis* octahedral geometry in the solid state, confirming that the solid-state structures are similar to those at room temperature in solution (Scheme 2) and in the crystalline state. As pointed out in Table 4, a monotonous decrease of the QS values is observed when putting a methyl group in ortho, meta or para position of the phenyl moiety. Two main reasons may be invoked to account for this behaviour: a modification of the electronic density imbalance around the tin nucleus, due to the donor effect of the methyl group, or a steric effect affecting the geometry of the tin centre. The steric contribution determining the C7—N—Sn angle distortion seems larger than the electronic influence, because the latter would lead to a sequence ortho, para, meta rather than the observed ortho, meta, para one for the QS values. The most remarkable structural feature in compounds **1–4** is their tendency to aggregate at high concentration in solution, whereas the structure remains monomeric in the solid state.

2.4 X-ray crystallography

The molecular structure of **3** is shown in Fig. 1 and selected interatomic parameters are collected in Table 5. The structure determination confirms the spectroscopic results showing a distorted trigonal bipyramidal geometry about the tin atom. In this description the axial positions are occupied by oxygen atoms derived from two monodentate carboxylate groups and the trigonal plane is defined by the tertiary amine nitrogen and two carbon atoms. The tin atom lies 0.0293(3) Å above the NC_2 plane in the direction of the O(3) atom. The distortion from the ideal axial angle for O—Sn—O may be traced to a significant extent to the strain induced by the formation of the bicyclic arrangement introduced by the tridentate mode of coordination adopted by the dianion. This effect is manifested in the acute O—Sn—N angles (Table 5). There is no evidence for additional interactions, either intra- or inter-molecular, to the tin atom. The closest intermolecular interactions involving tin, *i.e.* Sn—$O(2)^{i}$ and Sn—$O(4)^{ii}$ interactions are 4.297(4) Å and 4.433(4) Å respectively, lie well outside the sum of the van der Waals radii for these atoms; symmetry operations (*i*) $-x, -y, 1-z$ and (*ii*) $-x, -y, -z$.

Within the lattice the closest intermolecular interactions do indeed involve the non-coordinating carbonyl oxygen atoms. Thus, each of O(2) and O(4) exists in a pocket defined, in the first instance, by three methylene-type hydrogen atoms. The closest of these separations is found for the O(2) atom such that O(2)—H—$C(3)^{iii}$ is 2.30 Å and O(2)—$C(3)^{iii}$ is 3.130(5) Å; symmetry operation (*iii*) $x, \frac{1}{2}-y, \frac{1}{2}+z$. For the O(4) carbonyl atom, the closest interaction is 3.210(5) Å for O(4)—$C(2)^{iv}$, corresponding to a O(4)—H^{iv} contact of 2.44 Å; symmetry operation (*iv*) $x, \frac{1}{2}-y, -\frac{1}{2}+z$.

2.5 Mass spectrometric data

The 70 eV electron impact (EI) mass spectra of compounds **1–4** show a fragmentation pattern involving loss of *n*-Bu, and subsequently of CO_2, C_4H_8, R and H. The proposed fragmentation is

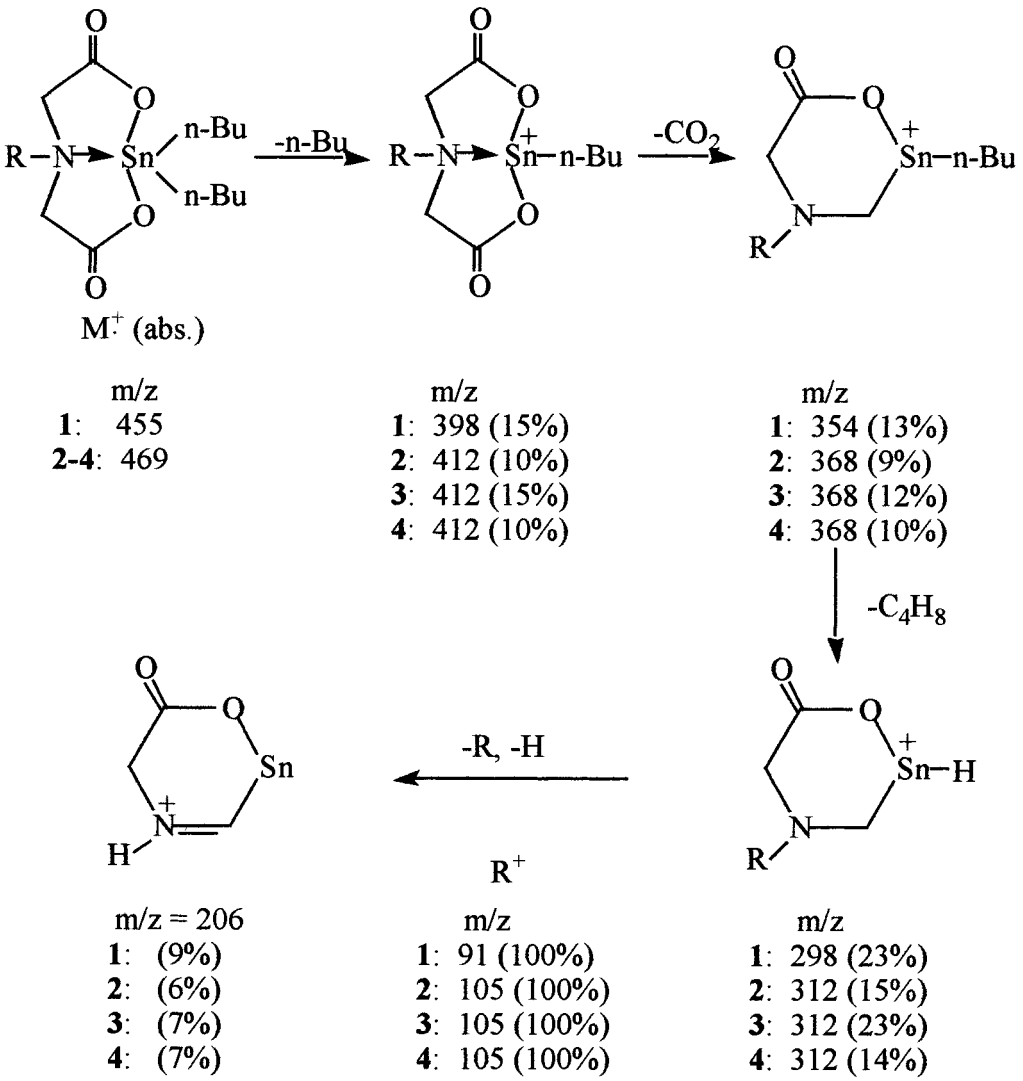

Scheme 3

shown in Scheme 3 and is comparable to those proposed for analogous compounds.[6,19]

2.6 Antitumour activity *in vitro*

The compounds **1–4** were screened *in vitro* against seven human cancer cell lines of human origin, MCF-7 and EVSA-T (mammary cancers), WiDr (colon cancer), IGROV (ovarian cancer), M19 MEL (melanoma), A498 (renal cancer) and H226 (lung cancer),[29,30] as well as against six more cell lines, two of astrocytic origin (U-87MG and U-373MG), two of colorectal origin (HCT-15 and LoVo) and two of pulmonary origin (A549 and A-427), according to a different protocol.[31,32]

The IC_{50} values of compounds **1–4** (Table 6) for the seven first cell lines are provided together with those of some clinically used reference compounds,[29,30] doxorubicin (DOX), cisplatin (CPT), 5-fluorouracil (5-FU), methotrexate (MTX) and etoposide (ETO), given for comparison. The screening results of Table 6 indicate that the compounds **1–4** are more active *in vitro* than cisplatin, 5-fluorouracil and etoposide. They are globally less active than doxorubicin except for

Table 6 *In vitro* inhibition concentrations IC_{50} (μM) of compounds **1–4** against seven tumour cell lines of human origin

	MCF-7	EVSA-T	WIDR	IGROV	M19 MEL	A 498	H226
1	0.12	0.10	0.45	0.15	0.18	0.15	0.16
2	0.11	0.10	0.64	0.13	0.18	0.13	0.18
3	0.12	0.10	0.59	0.16	0.17	0.15	0.16
4	0.11	0.10	0.38	0.13	0.12	0.10	0.13
DOX	0.02	0.01	0.02	0.10	0.03	0.16	0.35
CPT	2.3	1.4	3.2	0.6	1.9	7.5	10.9
5-FU	5.8	3.7	1.7	2.3	3.4	11	2.6
MTX	0.04	0.01	<0.005	0.02	0.05	0.08	5.0
ETO	4.2	0.52	0.24	0.96	0.83	2.2	6.5

MCF-7 (mammary cancer), EVSA-T (mammary cancer), WiDr (colon cancer), IGROV (ovarian cancer), M19 (melanoma), MEL A498 (renal cancer) and H226 (lung cancer). Reference compounds: DOX (doxorubicin), CPT (cisplatin), 5-FU (5-fluorouracil), MTX (methotrexate), ETO (etoposide).

IGROV, A498 and H226, for which they score comparably or even slightly better. They are also globally less active than methotrexate except for H226, against which the latter reference compound is, in comparison, strikingly less active. The substitution pattern of the aromatic ring has obviously no significant influence on the antitumour activity against these cell lines.

Table 7 shows that compounds **1–4** also decrease significantly to highly significantly the mean cellular proliferation of the six other cell lines studied.[31,32] They do not exhibit any cell specificity, even if compound **4** appears to be somewhat more active against A549, the other three compounds being less active against A549 than against the other five cell lines.

3. EXPERIMENTAL

3.1 Syntheses and characterization

Reagents were purchased from Aldrich Co.

The procedure used for the synthesis of compounds **1–4** consists of suspending bis(carboxymethyl)benzylamine (4.48 mmol) and di-*n*-butyltin oxide (4.48 mmol) in 200 ml of a refluxing ethanol/benzene 1/4 mixture for 6 h. The mixture becomes finally completely dissolved. The solvent mixture was evaporated under vacuum. The residue was dissolved in chloroform and precipitated with hexane to yield a white solid. Yields, m.p.: 98%, 169–171 °C (**1**); 85%, 176–178 °C (**2**); 93%, 167–168 °C (**3**); 95%, 172–174 °C (**4**). The IR spectra (KBr) show pairs of carbonyl stretching bands at 1638 and 1558 cm^{-1}, 1638 and 1576 cm^{-1}, 1640 and 1540 cm^{-1}, and 1640 and 1538 cm^{-1} for compounds **1** to **4** respectively, in agreement with literature data for similar compounds.[19] Elemental analysis data: Found (calc.) **1**: C, 50.22 (50.24); H, 6.52 (6.44); N, 3.23 (3.08). **2**: C, 50.83 (51.30); H, 6.87 (6.68); N, 3.14 (2.99). **3**: C, 51.04 (51.30); H, 6.62 (6.68); N, 3.11 (2.99). **4**: C, 49.84 (49.41); H, 6.74 (6.84); N, 2.98 (2.88). The presence of water in crystals of **4** has been evidenced by thermogravimetric analysis (TGA) coupled to mass spectrometry (MS) with a heated capillary transfer line.

Table 7 *In vitro* inhibition concentrations IC_{50} (μM) of compounds **1–4** against six tumour cell lines of human origin

	U-87MG	U-373MG	HCT-15	LoVo	A549	A-427
1	0.9	0.9	0.5	1	3	0.5
2	1	1	0.5	0.9	2	0.7
3	0.8	0.4	0.4	0.4	2	0.4
4	0.9	0.5	0.7	0.8	0.2	0.4

Cell lines of astrocytic origin: U-87MG and U-373MG; cell lines of colorectal origin: HCT-15 and LoVo; cell lines of pulmonary origin: A549 and A-427.

Table 8 Fractional atomic coordinates and U_{eq} values ($Å^2$) for non-hydrogen atoms in **3**

Atom	*x*	*y*	*z*	U_{eq} [a]
Sn	0.13928(2)	0.09733(2)	0.28387(2)	0.02989(6)
O(1)	0.0917(2)	0.0998(2)	0.4533(2)	0.0413(7)
O(2)	−0.0345(2)	0.1452(2)	0.5522(2)	0.0446(9)
O(3)	0.1032(2)	0.0881(2)	0.0991(2)	0.0317(7)
O(4)	−0.0104(2)	0.1335(2)	−0.0542(2)	0.0373(8)
N(1)	−0.0351(2)	0.1061(2)	0.2489(2)	0.0240(7)
C(1)	0.0008(3)	0.1338(3)	0.4617(3)	0.034(1)
C(2)	−0.0641(3)	0.1618(2)	0.3464(3)	0.0292(9)
C(3)	−0.0621(3)	0.1503(2)	0.1322(3)	0.030(1)
C(4)	0.0139(3)	0.1215(2)	0.0496(3)	0.029(1)
C(5)	−0.0774(3)	0.0075(2)	0.2498(3)	0.0243(9)
C(6)	−0.1957(3)	0.0013(2)	0.2251(3)	0.0256(9)
C(7)	−0.2466(3)	−0.0155(3)	0.1124(3)	0.034(1)
C(8)	−0.3545(3)	−0.0220(3)	0.0907(3)	0.043(1)
C(9)	−0.4137(3)	−0.0095(3)	0.1796(4)	0.043(1)
C(10)	−0.3656(3)	0.0067(3)	0.2922(3)	0.035(1)
C(11)	−0.2570(3)	0.0119(2)	0.3139(3)	0.0287(9)
C(12)	−0.4302(3)	0.0167(3)	0.3904(4)	0.050(1)
C(13)	0.2127(3)	−0.0335(3)	0.3098(4)	0.041(1)
C(14)	0.2537(3)	−0.0760(3)	0.2078(4)	0.038(1)
C(15)	0.3060(3)	−0.1691(3)	0.2341(5)	0.054(1)
C(16)	0.3437(5)	−0.2147(4)	0.1307(5)	0.077(2)
C(17)	0.1997(4)	0.2348(3)	0.2910(5)	0.055(1)
C(18)	0.2681(4)	0.2564(3)	0.1989(6)	0.074(2)
C(19)	0.3606(4)	0.1993(4)	0.1945(5)	0.070(2)
C(20)	0.4299(4)	0.2288(4)	0.1067(5)	0.073(2)

[a] U_{eq} is defined as one-third the trace of the orthogonalized U_{ij} tensor.

The TGA curve was obtained from a 2950 TGA-TA instrument purged with 120 ml min of helium. The MS instrument was a Balzers Thermostar. From the start of the measurement up to 70 °C, mass loss was exclusively due to water, as assigned by MS, whereas at higher temperatures both H_2O and CO_2 losses were evidenced.

3.2 Spectroscopy

The NMR spectra were acquired on a Bruker Avance DRX250 instrument equipped with a Quattro probe tuned to 250.13 MHz, 62.93 MHz and 89.15 MHz for ^1H, ^{13}C and ^{117}Sn nuclei respectively. Some other NMR data were acquired on Jeol GLX-270, Jeol Eclipse-400, Bruker Avance DPX300 and Bruker AMX500 spectrometers. ^1H and ^{13}C chemical shifts were referenced to the standard Me_4Si scale from respectively residual ^1H and ^{13}C–^2H solvent resonances of chloroform ($CHCl_3$, 7.23 ppm, and $CDCl_3$, 77.0 ppm, for ^1H and ^{13}C nuclei respectively). The ^{117}Sn resonance frequencies were referenced to $\Xi(^{117}Sn)$ 35.632 295 MHz.[27,28] 2D ^1H–^{13}C HMQC and HMBC correlation spectra as well as the 2D NOESY[23] and 2D off-resonance ROESY[24] spectra were acquired using the pulse sequence of the Bruker program library adapted to include gradient pulses,[33] as described recently.[34] The ^{117}Sn solid state CP-MAS NMR spectra were obtained as previously;[28] however, on a Bruker DRX250 instrument the ^{117}Sn rather than ^{119}Sn nucleus is used in order to overcome local radio interferences in the resonance frequency of the latter. Mass spectra were obtained on a Hewlett-Packard 59940-A instrument, and infrared spectra, on a Perkin-Elmer 16F PC FT-IR spectrometer.

Mössbauer data were acquired as described previously.[35]

3.3 Crystallography

Data for a colourless, thin plate ($0.03 \times 0.24 \times 0.37\ mm^3$) were collected at 173 K on a Rigaku AFC7R diffractometer with Mo -Kα radiation and the ω–2θ scan technique such that θ_{max}

was 27.5 °. The 5331 data were corrected for Lorentz and polarization effects[36] and an empirical absorption correction was applied.[37] Of the 5092 unique data, 3080 that satisfied the $I = 3.0\sigma(I)$ criterion were used in the subsequent analysis.

Crystal data: $C_{20}H_{31}NO_4Sn$, $M = 468.2$, monoclinic, $P2_1/c$, $a = 12.895(3)$, $b = 14.44(1)$, $c = 11.598(7)$ Å, $\beta = 98.55(3)$ °, $V = 2135(2)$ Å^3, $Z = 4$, $D_x = 1.456$ g cm^{-3}, $\mu = 12.19$ cm^{-1}, $F(000) = 960$.

The structure was solved by heavy-atom methods[38] and refined by a full-matrix procedure based on F.[36] Non-hydrogen atoms were refined with anisotropic displacement parameters and hydrogen atoms included in the model at their calculated positions. The refinement converged after the application of a weighting scheme of the form $w = 1/[\sigma^2(F) + 0.00021|F|^2]$ with $R = 0.032$ and $R_w = 0.037$. The maximum residual in the final difference map was 0.63 e Å^{-3}. Fractional atomic coordinates are listed in Table 8 and the numbering scheme used is represented in Figure 1, which was drawn with ORTEP.[39]

3.4 Antitumour screening protocols

The compounds were first screened against seven human cancer cell lines, from aqueous solutions containing 1% of DMSO or ethanol according to a protocol described previously (Table 5).[29,30] The IC_{50} values of some clinically used reference compounds, doxorubicin (DOX), cisplatin (CPT), 5-fluorouracil (5-FU), methotrexate (MTX) and etoposide (ETO), are given for comparison.

The screening method used for the data of Table 6 is that reported by Mosman[31] and modified by Carmichael *et al.*[32] It is based on the measurement of the number of living, metabolically active cells capable of transforming the yellow 3-(4,5-dimethylthiazol-2-yl)-2,5-diphenyl-tetrazolium bromide into the blue formazan by mitochondrial reduction.[40–42]

Acknowledgements The authors thank the 'Consejo Nacional de Ciencia y Tecnología (Conacyt-Mexico)' and the Universidad Autónoma Metropolitana (UAM-X) for a research scholarship (C.C.C.), and the 'Consejo Nacional de Ciencia y Tecnología (Conacyt)' for financial support (nos G32710E, 32198E) and a research scholarship (L.S.Z.R.). R.W., M.B. and M.G. are indebted to the Fund for Scientific Research Flanders (Belgium) for financial support [grants G.0192.98 (R.W., M.B.) and G.0074.00, (M.G.)]. M.K. thanks the 'Ministère de 1'Education Nationale du Luxembourg' (grant nos BFR93/051, BPU96/130, BPU97/138, BPU98/071) and the Action 'Vaincre le Cancer du Luxembourg'. The Australian Research Council is thanked for support of the crystallographic facility.

REFERENCES

1. Crowe AJ. The antitumour activity of tin compounds. In *Metal-Based Antitumour Drugs*, vol. 1, Gielen M (ed.). Freund Publ. House Ltd, London, 1988; 103–149.
2. Haiduc I, Silvestru C. *Organometallics in Cancer Chemotherapy. Main Group Metal Compounds*, vol. 1. CRC Press, Boca Raton, FL, 1989.
3. Gielen M. *Coord. Chem. Rev.* 1996; **151**: 41.
4. de Vos D, Willem R, Gielen M, van Wingerden KE, Nooter K. *Met. Based Drugs* 1998; **5**: 179.
5. Keppler BK (ed.). *Metal Complexes in Cancer Chemotherapy*. VCH, Weinheim, 1993; 351–390.
6. Meriem A, Gielen M, Willem R. *J. Organomet. Chem.* 1989; **365**: 91.
7. Gielen M, Bouâlam M, Meriem A, Mahieu B, Biesemans M, Willem R. *Heteroat. Chem.* 1992; **3**: 449.
8. Garrigues B. *Tetrahedron* 1994; **40**: 1151.
9. Mancilla T, Alarcón ML, Carrillo L. *Heteroat. Chem.* 1994; **5**: 455.
10. Mancilla T, Carrillo L, Reducindo MP. *Polyhedron* 1996; **15**: 3777.
11. Mancilla T, Contreras R, Wrackmeyer B. *J. Organomet. Chem.* 1986; **307**: 1.
12. Mancilla T, Höpfl H, Bravo G, Carrillo L. *Main Group Met. Chem.* 1997; **20**: 31.
13. Nardin G, Randaccio L, Bonomo R, Rizzarelli E. *J. Chem. Soc. Dalton Trans.* 1980; 369.
14. Castineira A, Abarca ME, De La Cueva I, González JM, Niclos J. *J. Coord. Chem.* 1993; **30**: 273.
15. Rodgers J, Jacobson RA. *Inorg. Chim. Acta* 1975; **13**: 163.
16. Mootz D, Wunderlich H. *Acta Crystallogn. Sect. B* 1980; **36**: 1189.
17. Dakternieks D, Dyson G, Jurkschat K, Tozer R, Tiekink ERT. *J. Organomet. Chem.* 1993; **458**: 29.
18. Meriem A, Gielen M, Willem R. *J. Organomet. Chem.* 1989; **365**: 91.
19. Tzschach A, Jurkschat K, Zschunke A, Mügge C. *J. Organomet. Chem.* 1980; **193**: 299.
20. Gielen M, Lelieveld P, de Vos D, Willem R. *In vitro* antitumour activity of organotin compounds. In *Metal-Based Antitumour Drugs*, vol. 2, Gielen M. (ed.) Freund Publ. House, Tel Aviv, 1992; 29–54.
21. Mancilla T, Carrillo L, Zamudio LS. Unpublished results.
22. HyperChem. Computational Chemistry, Version 5.02, 1996.
23. Jeener J, Meier BH, Bachmann P, Ernst RR. *J. Chem. Phys.* 1979; **71**: 4546.
24. Desvaux H, Berthault P, Birlirakis N, Goldman M, Piotto M. *J. Magn. Reson. A* 1995; **113**: 47.
25. Simons WW, (ed.). *The Sadtler Handbook of Proton NMR Spectra.* Heyden, London, 1978; 836–839.

26. Holecek J, Nádvorník M, Handlir K, Lycka A. *J. Organomet. Chem.* 1986; **315**: 299.
27. Gielen M, Dalil H, Ghys L, Boduszek B, Tiekink ERT, Martins JC, Biesemans M, Willem R. *Organometallics* 1998; **17**: 4259.
28. Willem R, Bouhdid A, Mahieu B, Ghys L, Biesemans M, Tiekink ERT, de Vos D, Gielen M. *J. Organomet. Chem.* 1997; **531**: 151.
29. De Vita Jr VT, Hellman S, Rosenberg SA, (eds). *Cancer: Principles and Practice of Oncology*, 5th ed. Lippincott-Raven Publ., Philadelphia, 1997.
30. Kepers YP, Peters GJ, Van Ark-Otte J, Winograd B, Pinedo HM. *Eur. J. Cancer* 1991; **27**: 897.
31. Mosman T. *J. Immunol. Meth.* 1983; **65**: 55.
32. Carmichael C, De Graff WG, Gazdar AF, Minna D, Mitchell B. *Cancer Res.* 1987; **47**: 936.
33. Keeler J, Clowes RT, Davis AL, Laue ED. *Methods Enzymol.* 1994; **239**: 145.
34. Willem R, Bouhdid A, Kayser F, Delmotte A, Gielen M, Martins JC, Biesemans M, Mahieu B, Tiekink ERT. *Organometallics* 1996; **15**: 1920.
35. Bouâlam M, Willem R, Biesemans M, Mahieu B, Meunier-Piret J, Gielen M. *Main Group Met. Chem.* 1991; **14**: 41.
36. TEXSAN: Structure Analysis Software. Molecular Structure Corp., The Woodlands, TX.
37. Walker N, Stuart D. *Acta Crystallogr. Sect. A* 1983; **39**: 158.
38. Beurskens PT, Admiraal G, Beurskens G, Bosman WP, García-Granda S, Smits JMM, Smykalla C. The DIRDIF program system, Technical Report of the Crystallography Laboratory, University of Nijmegen, The Netherlands (1992).
39. Johnson CK. ORTEP. Report ORNL-5138, Oak Ridge National Laboratory, TN, 1976.
40. Etiévant C, Kruczynski A, Pauwels O, Kiss R. *Anticancer Res.* 1991; **11**: 305.
41. Darro F, Kruczynski A, Etievant C, Martinez J, Pasteels J-L, Kiss R. *Cytometry* 1993; **14**: 783.
42. Darro F, Camby I, Kruczynski A, Pasteels JL, Martinez J, Kiss R. *Gut* 1995; **36**: 220.

